Int. J. Electrochem. Sci., 12 **(2017)** 1064 – 1074, doi: 10.20964/2017.02.21

International Journal of
ELECTROCHEMICAL
SCIENCE
www.electrochemsci.org

F-doped TiO_2 Compact Film for High-Efficient Perovskite Solar Cells

M. Che[1], *Y. Fang*[1], *J. Yuan*[1], *Y. Zhu*[1], *Q. Liu*[2], *J. Song*[1,*]

[1] School of Materials Science and Engineering, China University of Mining and Technology, Xuzhou 221116, China
[2] Department of Chemical and Biomedical Engineering, West Virginia University, Morgantown, West Virginia 26506, United States
[*]E-mail: jsoong@cumt.edu.cn

Received: 8 November 2016 / *Accepted:* 11 December 2016 / *Published:* 30 December 2016

The high quality compact layer plays a crucial role in electron transport and hole blocking in perovskite solar cells (PSCs). In this study, F-doped TiO_2 dense layer was utilized to enhance the electron mobility and conductivity of the compact layer. Upon optimization of F doping content, the device with 3% F-doped TiO_2 compact layer achieves outstanding power conversion efficiency (PCE) of 14.12%, increased by about 13% compared with the one using pure TiO_2 compact layer. Scanning electron microscopy (SEM) showed that the dense and homogeneous TiO_2 layer had a thickness of about 30 nm. Direct current conductivity measurement revealed the enhanced electron conductivity of F-doped TiO_2 layer. Moreover, the photoluminence (PL) spectra were employed to demonstrate the improved electron transfer process at F-doped TiO_2/perovskite interface.

Keywords: F-doped TiO_2, compact layer, perovskite solar cell

1. INTRODUCTION

Since an organometal halide was synthesized by Miyasaka [1], perovskite solar cells (PSCs) have attracted enormous amount of attentions in the field of photovoltaic technology in last few years. Based on the inherent advantages of lead halide perovskite materials such as high carrier mobility, low exciton bonding energy, and long electron-hole diffusion lengths [2-6], many devices with high power conversion efficiency (PCE) have been obtained via various strategies [7-10]. In particular, the excellent PCE of 22% has been certified recently [11], and the ascent rate is much higher than dye-sensitized solar cell [12-14].

In the PSCs architectures, the quality of the compact layer plays a crucial role for electron transport in the perovskite devices [15, 16]. The main methods to prepare electron transport layer include spin-coating [17, 18], spray pyrolysis [19, 20], atomic layer deposition [21-23] and thermal oxidation [24]. Specially, spray pyrolysis is outstanding among these methods due to its advantages of simple operation and high efficiency. Up to now, many attentions have been focused on electron transport layer materials to obtain a film with high carrier mobility, suitable conduction band and compact morphology. Compared with traditional TiO_2, some new transition metal oxides, such as ZnO or SnO_2, also present excellent features as compact layers [25-29]. In addition, material for the compact layer was also modified via doping with other components. Nb-doped TiO_2 compact layer was used in PSCs with a high PCE of 16.3%, which was mainly attributed to the diminished selective contact resistance and enhanced charge recombination resistance [3]. The Y-doped TiO_2 was also applied to fabricate compact layer and the PCE of 19.3% in planar PSCs devices was confirmed by Yang's group [30].

In this study, the homogeneous F-doped TiO_2 dense layer were prepared to fabricate efficient PSCs. We found that F doping in TiO_2 led to an enhancement of short-circuit current density for PSCs. Under optimized doping content, the cell achieved a PCE of 14.12%, increased by 13% compared with the one employing pure TiO_2 compact film. Further research indicated that the enhancement originated from the facilitated electron injection and extraction, which was characterized via direct current conductivity and photoluminence (PL) spectra.

2. EXPERIMENTAL

2.1 Device fabrication

F-doped SnO_2 (FTO, 2.2 mm thick, <15 ohm/sq, Opvtech) glass substrates were etched with the turbid solution of Zn powder and concentrated hydrochloric acid. Then, the patterned FTO was cleaned under ultrasonication for 30 min in ethanol and isopropanol, successively [31]. For the preparation of TiO_2 compact layer, the diluted titanium diisopropoxide bis(acetylacetonate) solution (1:100 by volume in isopropanol) were sprayed on the clean FTO glass substrate at 450 °C. For doping, titanium tetrafluoride (TiF_4) was added in the above solution and the atom ratios of F to Ti were defined to 1%, 3%, 5%, and 10%. Subsequently, a TiO_2 paste (Dyesol 18 NRT) was spin-coated on the TiO_2 compact layer at 5000 rpm for 30s, and then annealed at 500 °C for 15 min in a furnace under ambient air. The perovskite layer was fabricated by two step spin-coating method. 1.3 mol/L PbI_2(DMSO) solution in N,N-dimethylformamide (DMF) was prepared at 70 °C, which was dropped onto the mesoporous TiO_2 film after infiltration and spin-coated at 3000 rpm for 30 s. Then 200 μL methylammonium iodide in isopropanol (CH_3NH_3I, MAI, 15 mg/mL) was spin coated on the PbI_2(DMSO) film at 5000 rpm for 30 s and then annealed at 150 °C for 20 min in glove box. The white powder of MAI was synthesized according to early reports [17, 32]. After cooling to room temperature, 50 μL hole transport material (HTM) solution was spin-coated on the perovskite layer at 3000 rpm for 30 s. The HTM solution was prepared by dissolving 72.3 mg (2,2',7,7'-tetrakis(N,N-di-

p-methoxyphenylamine)-9,9-spirobifluorene) (spiro-MeOTAD), 28.8μL 4-tert-butylpyridine (TBP), 17.5 μL of bis(trifluoromethylsulphonyl) imide (LiTFSI) in acetonitrile (520 mg/mL) in 1 mL chlorobenzene. Finally, the 55 nm of Ag as counter electrode was evaporated using thermal evaporator on the HTM-coated film.

2.2 Characterization

The X-ray photoelectron spectroscopy (XPS) was conducted with a photoelectron spectrometer (ESCALAB 250Xi, Thermo Fisher Scientific). The morphology of compact thin films and $CH_3NH_3PbI_3$ film were characterized by field-emission scanning electron microscopy (FESEM, 1530VP, LEO). The UV-visible transmittance spectra (UV-Vis) of different TiO_2 compact films were recorded by a spectrophotometer (Cary-300 spectrometer, Varian). The current density-voltage (J-V) curves of perovskite solar cells were carried out by an electrochemical workstation (IM6ex, Zahner), and the devices were illuminated by a solar simulator (Oriel Sol 3A, Newport) under 100 mW cm^{-2} irradiation. The aperture area of devices was controlled at 0.1 cm^2 by a metal mask during the measurement. The incident photon-to-electron conversion efficiency (IPCE) spectrum for perovskite solar cells were measured by a Newport IPCE system (Newport, USA).

3. RESULTS AND DISCUSSION

A dense TiO_2 layer has a critical role in perovskite solar cell for current-leakage suppression. As shown in Fig. 1a, the TiO_2 film exhibited a dense image without any pinholes. As the small thickness of the TiO_2 film (30 nm), the surface morphology basically replicated the underlying FTO morphology, as shown in Fig. 1b. Besides, as presented in Fig. 1c, the perovskite layer deposited on TiO_2 mesoporous film was uniform and dense which had a crystal size of 200-500 nm.

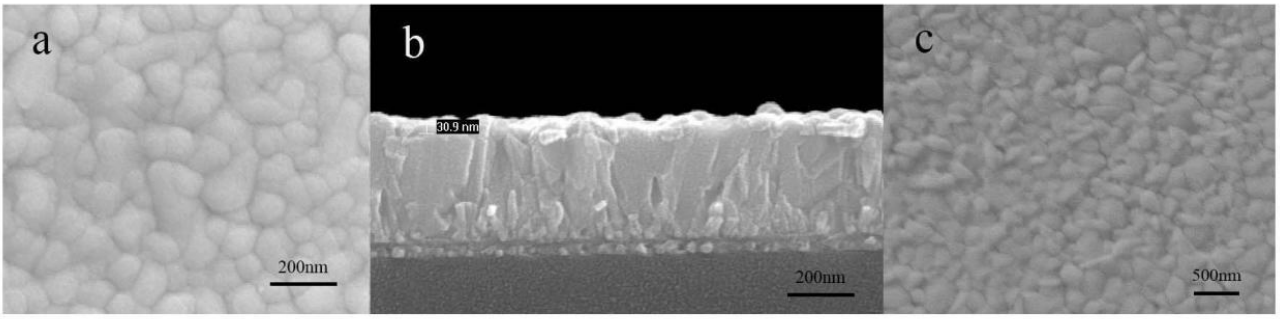

Figure 1. (a) Top-view and (b) cross-sectional SEM images of 3% F-doped TiO_2 film on FTO substrate. (c) SEM image of $CH_3NH_3PbI_3$ deposited on 3% F-doped TiO_2 compact layer.

The X-ray photoelectron spectroscopy (XPS) analysis was carried out to demonstrate the chemical element change with introducing fluorine. Fig.2 showed the XPS spectra of 5% F-doped

TiO_2 compact film based on blank glass instead of FTO substrate to avoid the interference of fluorine in FTO. As presented in Fig.2a, two core level peaks, Ti $2p_{1/2}$ and Ti $2p_{3/2}$, at binding energies of 457.5 and 463.5 eV clearly indicated the Ti^{4+} state, which was in consistent with a previous report [3]. In addition, the F1s state with binding energy of 683 eV (Fig.2b) confirmed that F was indeed doped into the TiO_2 compact layer.

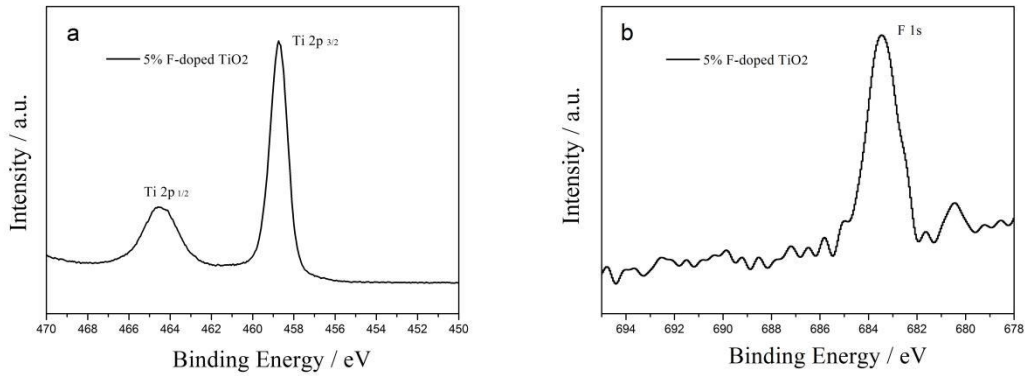

Figure 2. XPS spectra of (a) Ti and (b) F in F-doped TiO_2 compact layer.

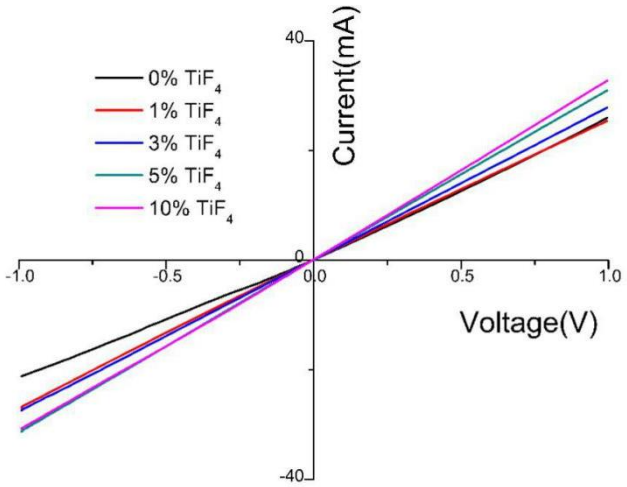

Figure 3. I–V curves of FTO/ TiO_2 compact layer /Ag devices.

To investigate the direct current conductivity (σ_0) of the compact films with different amounts of F dopant, a simple device configuration of FTO/TiO_2 compact layer/Ag was fabricated, where the evaporated Ag film played a role of contact electrode. Fig. 3 presented the typical current-voltage (I-V) characteristics curves of the devices with various F dopants. According to the relationship between current and voltage,

$$I = \sigma_0 A D^{-1} V$$

where A is the area (25.5 mm^2) and D is the thickness (50 nm) of the device. The calculated σ_0 values were displayed in Table 1. For comparison, we found a tendency that the direct current conductivity enhanced with the increase of F dopants. According to the literature [33], the reason for

this phenomenon may be ascribed to the fact that the coordination of Ti^{4+} and O^{2-} in TiO_2 crystal lattice was replaced with F ion, and an extra electron was produced in the substituted position. Meanwhile, a defect energy level whose position was lower than the TiO_2 conduction band was formed [34], leading to an increased σ_0.

Table 1. The calculated direct current conductivity of F-doped TiO_2 films with different F concentrations.

	$\sigma_0 / mS \cdot cm^{-1}$
0% F-TiO_2	4.34568×10^{-3}
1% F-TiO_2	4.47255×10^{-3}
3% F-TiO_2	5.44902×10^{-3}
5% F-TiO_2	6.02941×10^{-3}
10% F-TiO_2	6.23529×10^{-3}

Optical property of TiO_2 films after doping is important as a high transparency allows a large photon flux to reach the perovskite layer for photocurrent generation. As seen in the Fig. 4, all TiO_2 films had good transparency (over 80%) in the range from 500 to 900 nm. Nonetheless, transmittances of TiO_2 films were reduced as the increase of F doping amounts. Thus, excess F dopant was unfavorable for photovoltaic performance of PSCs.

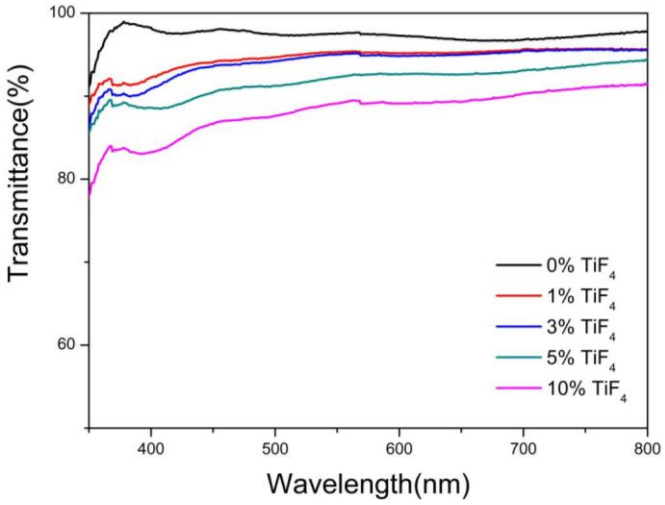

Figure 4. UV-Vis transmittance spectra of F-doped TiO_2 films with different F concentrations.

The *J-V* curves of PSCs with different compact layers were displayed in Fig. 5, and the relevant parameters including short-current density (J_{sc}), open-circuit voltage (V_{oc}), fill factor (FF) and (PCE)

were recorded in the Table 2. Devices using pure TiO_2 compact layer yielded relatively low PCE of 12.52%. In contrast, after F^- was introduced, especially for 3% F-doped TiO_2, the photovoltaic performance of PSC device was significantly improved, causing J_{sc} of 19.40 mA/cm^2, V_{oc} of 1.01 V, FF of 72.31%, and PCE of 14.12%. Obviously, the enhancement of PCE with F-doped TiO_2 compact layer could be mainly attributed to the increase of J_{sc}. The pronounced increase in σ_0 after F doping could be the main reason for the *Jsc* enhancement, as demonstrated in Table 1, which was benefit for electron extraction and transport. However, as F content increased further to 5%, the performance of device had a descending trend. Moreover, the PSC based on 10% F-doped TiO_2 film had conversion efficiency as low as 11.09%. The decreased PCE might be attributed to the low transparency of TiO_2 compact film after F doping.

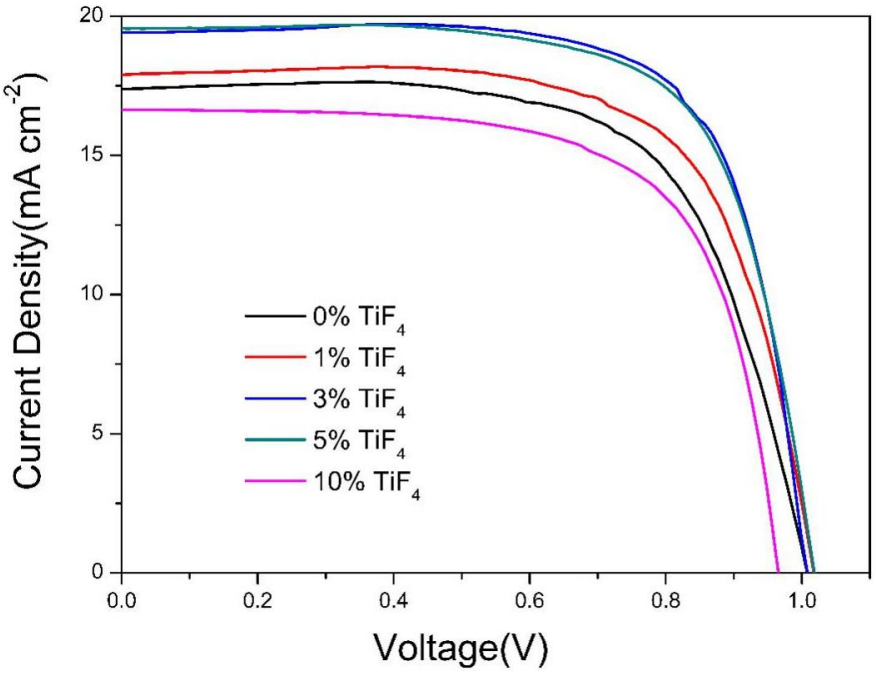

Figure 5. The current density-voltage (*J-V*) curves of PSCs based on different compact film. All the devices were measured under illumination of 100 mW cm^{-2} and active area of 0.1cm^2.

Table 2. Photovoltaic parameters of the best-performing PSCs with different F-doped TiO_2 compact layers.

samples	J_{sc} (mA/cm^2)	V_{oc} (v)	FF (%)	PCE (%)
TiF_4:TiO_2=0%	17.16	1.04	70.08	12.52
TiF_4:TiO_2=1%	17.77	1.02	70.32	12.68
TiF_4:TiO_2=3%	19.40	1.01	72.31	14.12
TiF_4:TiO_2=5%	19.54	1.02	70.21	13.96
TiF_4:TiO_2=10%	17.09	0.93	67.67	11.09

The incident photon-to-current conversion efficiency (IPCE) spectra with different compact films were also depicted in Fig. 6. We could see that a clear absorption began at 780 nm, which was matched with the band gap of $CH_3NH_3PbI_3$ [19]. Besides, compared with the device without F doping, the device with 3% F-doped TiO_2 compact layer exhibited higher quantum yield in the range from 310 to 780 nm, which was agreed with the higher J_{sc} of corresponding PSCs.

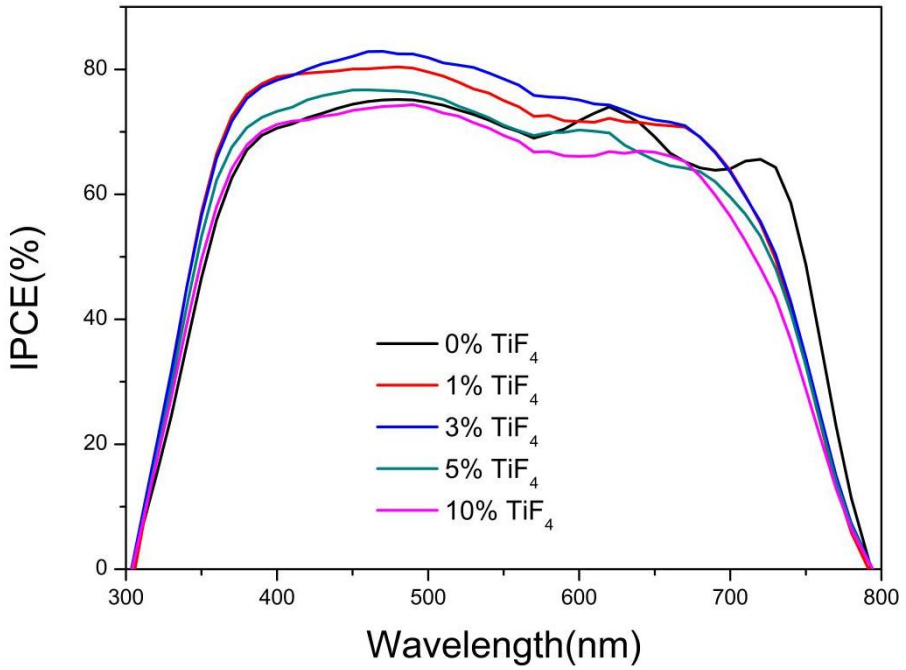

Figure 6. The IPCE spectra for PSCs based on different F contents in TiO_2 compact films.

To illustrate the charge transfer process at TiO_2/perovskite interface in the device, steady-state photoluminescence (PL) of samples with configurations of glass/compact TiO_2/mesoporous TiO_2/ perovskite were measured. Fig. 7 displayed the steady-state PL spectra of perovskite with different F-doped TiO_2 compact layers. An intensive photoluminescence peak appears at 770 nm, and an obvious PL quench appeared when TiO_2 compact layer was doped with 1%-5% fluorine. This phenomenon indicated that the recombination of light-excited electrons and holes at TiO_2/perovskite interface was restrained effectively after F doping [35]. This was the main reason for photovoltaic performance enhancement in PSCs employing F-doped TiO_2 compact layer. However, the PL intensity of sample using 10% F-doped TiO_2 film showed apparent enhancement compared with others. The excessive amounts of F in TiO_2 film might provide many defects and lead to serious charge recombination in the process of electron transport. This disadvantage for electron transfer combined with the low transparency as F doping in TiO_2 compact film led to the decreased photovoltaic performance of corresponding PSC device.

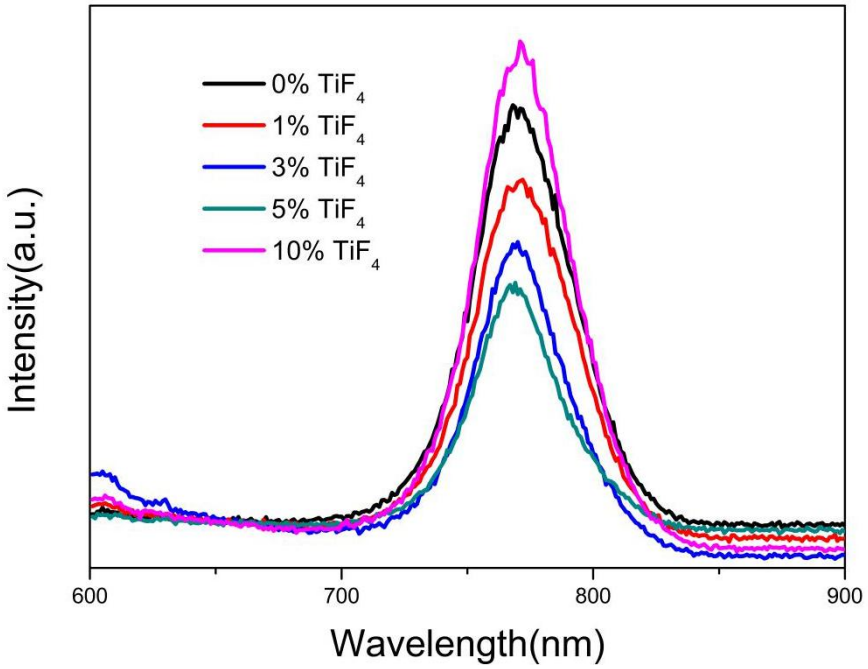

Figure 7. The PL spectra of glass/ F-doped TiO_2/m-TiO_2/$CH_3NH_3PbI_3$ films.

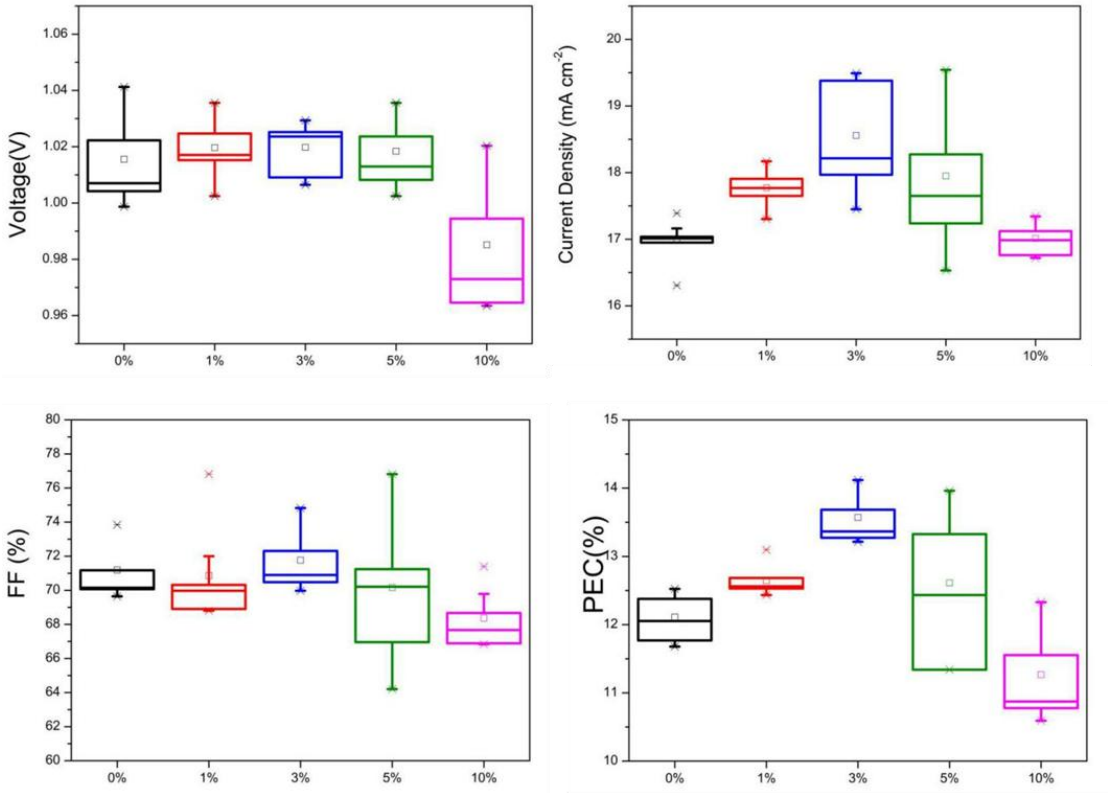

Figure 8. Statistical values of Voc, Jsc, FF, and PCE of perovskite solar cells using different compact layers in 10 independent devices.

Additionally, we recorded distribution of photovoltaic performance of PSCs using different compact layers in Fig. 8. The average values of photovoltaic parameters including Jsc, Voc, FF, and

conversion efficiency increased gradually as the F dopant amounts turned from 0 to 3%. However, these parameters went down as the F dopant amounts increased further to 5% and 10%. The PSC based on 3% F-doped TiO_2 compact layer presented the highest average photovoltaic performance, and the values distributions were relatively concentrated than other ones. This property was benefit to fabricate PSCs with good reproducibility.

Table 3. Photovoltaic performance of perovskite solar cells based on mesoporous structures in literatures using different dopants in TiO_2 compact layer.

Dopant	η (%) (pristine TiO_2)	η' (%) (doped TiO_2)	$(\eta'-\eta)/\eta$ (%)
Magnesium (Mg) [36]	9.81	12.81	30.6
Niobium (Nb) [37]	9.22	10.26	11.3
Fluorine (F)[This work]	12.52	14.12	12.8

To evaluate the capability of fluorine dopant in TiO_2 compact film, we compared our results with some similar literatures. As the varied fabrication process of perovskite solar cell in different research groups, the basic photovoltaic performances of perovskite solar cells were different. In fact, the increase rate of conversion efficiency ($\Delta\eta/\eta$) was meaningful for comparison among different doping systems. The growth rate in our work was 12.8%, which was higher than Nb-doped one and lower than Mg-doped one. In other words, fluorine dopant could play comparable ability in enhancing photovoltaic performance of PSC with metal ions.

4. CONCLUSIONS

In conclusion, we successfully introduced the F ion into TiO_2 solution and sprayed it on FTO substrate to achieve homogeneous and high quality compact film for perovskite solar cells. After optimization, the 3% F doping contents was applied to fabricate the high efficiency perovskite solar cells (PSCs) with PCE of 14.12% and J_{sc} of 19.40 mA/cm^2. Further study indicated that the F doping contributed to impressive advances of film conductivity. Moreover, moderate F doping also would be conducive to enhanced PL quenching and achieve a high V_{oc}. The comprehensive information showed us that F doping for TiO_2 compact layer was an effective strategy for high-efficient perovskite solar cells.

ACKNOWLEDGEMENTS
We appreciate the financial supports from the Fundamental Research Funds for the Central Universities (2015QNA06).

References

1. A. Kojima, K. Teshima, Y. Shirai and T. Miyasaka, *J. Am. Chem. Soc*., 131 (2009) 6050.
2. T. C. Sum and N. Mathews, *Energy Environ. Sci*., 7 (2014) 2518.

3. B. X. Chen, H. S. Rao, W. G. Li, Y. F. Xu, H. Y. Chen, D. B. Kuang and C. Y. Su, *J. Mater. Chem.* A, 4 (2016) 5647.
4. J. H. Im, C. R. Lee and J. W. Lee, *Nanoscale*, 3 (2011) 4088.
5. G. C. Xing, N. Mathews and S. Y. Sun, *Science*, 342 (2013) 344.
6. S. D. Stranks, G. E Eperon, G. Grancini, C. Menelaou1, T. Leijtens, L. M. Herz, A. Petrozza and H. J. Snaith, *Science*, 342 (2013) 341.
7. D. Y. Son, J. W. Lee, Y. J. Choi, I. H. Jang, S. Lee, P. J. Yoo, H. Shin, N. Ahn, M. Choi, D. Kim and N. G. Park, *Nat. Energy*, 1 (2016) 16081.
8. M. M. Lee, J. Teuscher, T. Miyasaka, T. N. Murakami and H. J. Snaith, *Science*, 338 (2012) 643.
9. W. S. Yang, J. H. Noh, N. J. Jeon, Y.C. Kim, S. Ryu, J. Seo and S. Seok, *Science*, 348 (2015) 1234.
10. N. J. Jeon, J. H. Noh, W. S. Yang, Y. C. Kim, S. Ryu, J. Seo and S. Seok, *Nature*, 517 (2015) 476.
11. http://www.nrel.gov/ncpv/images/efficiency_chart.jpg.
12. L. Zhu, Y. H. Qiang, Y. L. Zhao and X. Q. Gu, *Appl. Surf. Sci*., 292 (2014) 55.
13. X. P. Lin, D. M. Song, X. Q. Gu, Y. L. Zhao and Y. H. Qiang, *Appl. Surf. Sci*., 263 (2012) 816.
14. Y. L. Zhao, D. M. Song, Y. H. Qiang, X. Q. Gu, L. Zhu and C. B. Song, *Appl. Surf. Sci*., 309 (2014) 85.
15. L. Cojocaru, S. Uchida, Y. Sanehira, J. Nakazaki, T. Kubo and H. Segawa, *Chem. Lett*., 44 (2015) 674.
16. M. H. Li, P. S. Shen, K. C. Wang, T. F. Guo and P. Chen, *J. Mater. Chem.* A, 3 (2015) 9011.
17. Y. Yang, J. Song, Y. L. Zhao, L. Zhu, X. Q. Gu, Y. Q. Gu, M. Che and Y. H. Qiang, *J. Alloy. Compd.*, 684 (2016) 84.
18. T. S. Su, T. Y. Hsieh, C. Y. Hong and T. C. Wei, *Sci. Rep*., 5 (2015) 16098.
19. J. Cui, F. P. Meng, H. Zhang, K. Cao, H. L. Yuan, Y. B. Cheng, F. Huang and M. K. Wang, *ACS Appl. Mater. Interfaces*, 6 (2014) 22862.
20. J. N. Hart, D. Menzies, Y. B. Cheng, G. P. Simon and L. Spiccia, C. R. Chim., 9 (2006) 622.
21. H. P. Dong, Y. Li, S. F. Wang, W. Z. Li, N. Li, X. D. Guo and L. D. Wang, *J. Mater. Chem.* A, 3 (2015) 9999.
22. Y. Z. Wu, X. D. Yang, H. Chen, A. Islam, P. Zhang and L.Y. Han, *Appl. Phys. Express*, 7 (2014) 52301.
23. A. K. Chandiran, A. Yella, M. T. Mayer, P. Gao, M. K. Nazeeruddin and M. Grätzel, *Adv. Mater*., 26 (2014) 4309.
24. W. J. Ke, G. J. Fang, J. Wang, P. L. Qin, H. Tao, H. W. Lei, Q. Liu, X. Dai and X. Z. Zhao, *ACS Appl. Mater. Interfaces*, 6 (2014) 15959.
25. D. Y. Son, J. H. Im, H. S. Kim and N. G. Park, *J. Phys. Chem*. C, 118 (2014) 16567.
26. K. Wang, Y. T. Shi, Q. S. Dong, Y. Li, S. F. Wang, X. F. Yu, M. Y. Wu and T. L. Ma, *J. Phys. Chem. Lett*., 6 (2015) 755.
27. W. J. Ke, G. J. Fang, J. Wang, P. L. Qin, H. Tao, B. L. Li, J. W. Wan, G. Yang and Y. F. Yan, *J. Am. Chem. Soc.*, 137 (2015) 6730.
28. P. Chen, X. T. Yin, M. Que, Y. W. Yang and W. X. Que, *RSC Adv*., 6 (2016) 57996.
29. Y. Li, J. Zhu, Y. Huang, F. Liu, M. Lv, S. H. Chen, L. H. Hu, J. W. Tang, J. Yao and S. Dai, *RSC Adv.*, 5 (2015) 28424.
30. H. P. Zhou, Q. Chen, G. Li, S. Luo, T. B. Song, H. S. Duan, Z. Hong, J. B. You, Y. S. Liu and Y. Yang, *Science*, 345 (2014) 542.
31. B. G. Zhao, L. Zhu, Y. L. Zhao, Y. Yang, J. Song, X. Q. Gu, Z. Xing and Y. H. Qiang, *J. Mater. Sci. - Mater. Electron.*, 27 (2016) 10869.
32. M. Che, L. Zhu, Y. L. Zhao, D. S. Yao, X. Q. Gu, J. Song and Y. H. Qiang, *Mater. Sci. Semicond. Process*., 56 (2016) 29.
33. Y. Y. Lv, L. S. Yu, H. Y. Huang, H. L. Liu and Y. Y. Feng, *Appl. Surf. Sci*., 255 (2009) 9548.

34. W. Yu, X. J. Liu, L. Pan, J. L. Li, J. Y. Liu, J. Zhang, P. Li, C. Chen and Z. Sun, *Appl. Surf. Sci*., 319 (2014) 107.
35. J. Song, S. P. Li, Y. L. Zhao, J. Yuan, Y. Zhu, Y. Fang, L. Zhu, X. Q. Gu and Y. H. Qiang, *J. Alloy. Compd.*, 694 (2017) 1232.
36. J. Wang, M. C. Qin, H. Tao, W. J. Ke, Z. Chen, J. W. Wan, P. L. Qin, L. B. Xiong, H. W. Lei, H. Q. Yu and G. J. Fang, *Appl. Phys. Lett.*, 106 (2015) 121104.
37. X. Yin, Y. J. Guo, Z. S. Xue, P. Xu, M. He and B. Liu, *Nano Res.*, 8 (2015) 1997.